VYSOKÉ UČENÍ TECHNICKÉ V BRNĚ

BRNO UNIVERSITY OF TECHNOLOGY

FAKULTA CHEMICKÁ

ÚSTAV CHEMIE MATERIÁLŮ

FACULTY OF CHEMISTRY
INSTITUTE OF MATERIAL SCIECE

PHOTOVOLTAIC PROPERTIES OF MOLECULES WITH INTERNAL CHARGE TRANSFER

FOTOVOLTAICKÉ VLASTNOSTI MOLEKUL S VNITŘNÍM PŘENOSEM NÁBOJE

BAKALÁŘSKÁ PRÁCE

BACHELOR´S THESIS

AUTOR PRÁCE   MAREK ŠENKÝŘ
AUTHOR

VEDOUCÍ PRÁCE   doc. Mgr. Martin Vala, Ph.D.
SUPERVISOR

BRNO 2015

Zadání bakalářské práce

Číslo bakalářské práce:	**FCH-BAK0858/2014**	Akademický rok:	**2014/2015**
Ústav:	Ústav chemie materiálů		
Student(ka):	**Marek Šenkýř**		
Studijní program:	Chemie a chemické technologie (B2801)		
Studijní obor:	Chemie, technologie a vlastnosti materiálů (2808R016)		
Vedoucí práce	**doc. Mgr. Martin Vala, Ph.D.**		
Konzultanti:			

Název bakalářské práce:

Fotovoltaické vlastnosti molekul s vnitřním přenosem náboje

Zadání bakalářské práce:

Práce je zaměřena na studium donor-akceptorových molekul s vnitřním přenosem náboje z hlediska jejich použití v organických solárních článcích. V práci bude studován vliv změny chemické struktury těchto molekul na optické a optoelektrické vlastnosti. Dále budou z těchto materiálů připraveny solární články a studováno jejich fotovoltaické chování.

Termín odevzdání bakalářské práce: 22.5.2015

Bakalářská práce se odevzdává v děkanem stanoveném počtu exemplářů na sekretariát ústavu a v elektronické formě vedoucímu bakalářské práce. Toto zadání je přílohou bakalářské práce.

-     -   -

      Marek Šenkýř   doc. Mgr. Martin Vala, Ph.D.   prof. RNDr. Josef Jančář, CSc.

       Student(ka)   Vedoucí práce   Ředitel ústavu

- -

V Brně, dne 30.1.2015   prof. Ing. Martin Weiter, Ph.D.

                                                         Děkan fakulty

ABSTRACT

The work is focused on the study of donor-acceptor molecules with internal charge transfer in terms of their use in organic solar cells. The work will be studied the effect of changes in the chemical structure of these molecules on the optical and optoelectronic properties. Furthermore, based on these materials prepared solar cells and photovoltaic studied their behavior.

Práce je zaměřena na studium donor-akceptorových molekul s vnitřním přenosem náboje z hlediska jejich použití v organických solárních článcích. V práci bude studován vliv změny chemické struktury těchto molekul na optické a optoelektrické vlastnosti. Dále budou z těchto materiálů připraveny solární články a studováno jejich fotovoltaické chování.

KEYWORDS

ŠENKÝŘ, M. *Fotovoltaické vlastnosti molekul s vnitřním přenosem náboje*. Brno: Vysoké učení technické v Brně, Fakulta chemická, 2015. 45 s. Vedoucí bakalářské práce do. Mgr. Martin Vala, Ph.D.

I declare that the diploma/bachelor thesis has been worked out by myself and that all the quotations from the used literary sources are accurate and complete. The content of the diploma/bachelor thesis is the property of the Faculty of Chemistry of Brno University of Technology and all commercial uses are allowed only if approved by both the supervisor and the dean of the Faculty of Chemistry, BUT

Marek Šenkýř

CONTENTS

THEORETICAL PART

1.1 WHY SOLAR ENERGY?

A majority of the world´s current electricity supply is generated from non-renewable resources and fossil fuels such as coal, oil and gases or nuclear power. The sources of this traditional energy cause world pollution, wars and poverty in many places. Prices of fossil fuels are adjusted by owning states and with a decline in world reserves price increases, of course [1].

The other ways how to make energy is renewable energy. It is energy naturally refreshed during their use. This is the energy flows that occur naturally close to the ground, and supplies that are renewed at least as fast as they are consumed.

For several billion years a thermonuclear reaction has been occurring on the Sun. The reaction converts solar hydrogen (which is not updated) into helium while releasing large amounts of energy. The solar energy is transmitted to Earth in the form of radiation. Energy input from the sun is, given the distance to the Earth, about 1,300 W/ m^2. This power is called the solar constant. On the territory of the Czech Republic falls on average 1100 kWh/ m^2 per year [2].

The current social structure and everyday life is closely connected with electricity. Our dependence on a stable supply of electric current is greater than many people realize, which proves increasingly frequent black outs that are able to paralyze entire countries for several days. This electricity, generally speaking energy, is slowly becoming a key strategic resource.

Nowadays scientists slowly gain knowledge of how to use this energy. This research focuses on the development of materials which would allow the transformation of solar energy into the electricity and could take an advantage of the huge potential that the sun provides us. This gives us some possibility to solve this not very positive trend of exploitation of non-renewable resources.

Currently this task lies on our shoulders, the questions are whether we can use this power at all, by what means do we want to achieve it and how much it will change future.

1.2 ORGANIC PHOTOVOLTAIC SYSTEM

Organic Photovoltaic (OPV) devices convert solar energy to electrical energy. A typical OPV device consists of one or several photo-active materials sandwiched between two electrodes. Figure 1 depicts a typical bi-layer organic photovoltaic device.
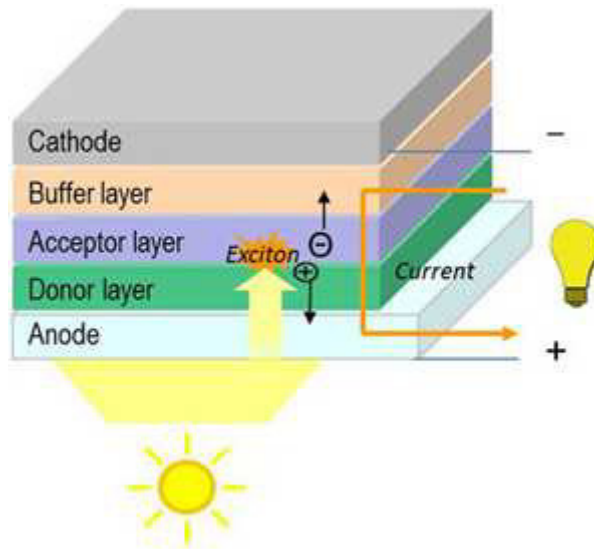
Figure 1 Structure of a bilayer organic photovoltaic device.

In OPV cell, sunlight is absorbed in the photo-active layers composed of donor and acceptor semiconducting organic materials to generate photo-currents. The donor material (D) donates electrons and mainly transports holes and the acceptor material (A) withdraws electrons and mainly transports them. As depicted in Figure 2, those photo-active materials harvest photons from sunlight to excite electrons, which form exciton from the valence band into the conduction band (Light Absorption). Due to the concentration gradient, the exciton diffuse to the donor/acceptor interface (Exciton Diffusion) and separate into free holes (positive charge carriers) and electrons (negative charge carriers) (Charge Separation). A photovoltaic is generated when the holes and electrons move to the corresponding electrodes by following either donor or acceptor phase (Charge Extraction) [3].
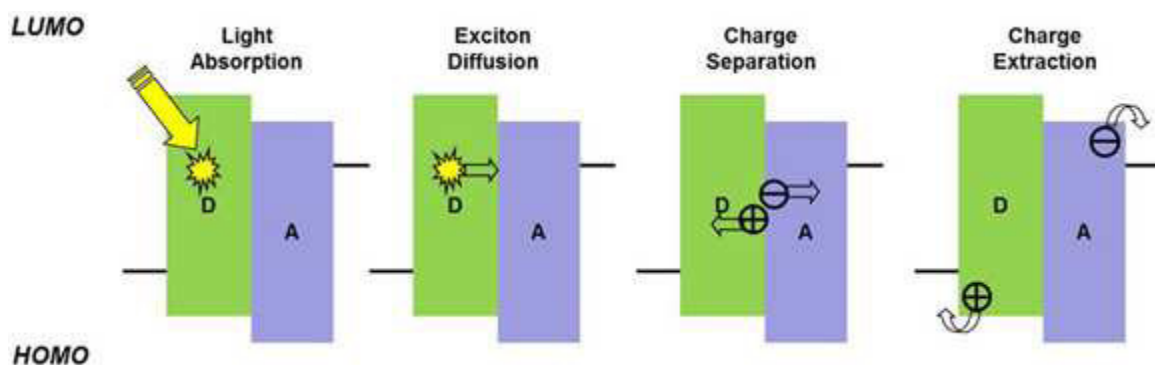

Figure 2 Functional mechanism of a bilayer organic photovoltaic (D = donor, A = acceptor).

Bulk hetero-junctions have an absorption layer consisting of a nanoscale blend of donor and acceptor materials. The large donor-acceptor inter-facial area results in a higher likelihood for the short-lived exciton to reach an interface and dissociate [4].

Bulk hetero-junctions have an advantage over layered photo-active structures because they can be made thick enough for effective photon absorption without the difficult processing involved in orienting a layered structure.

Bulk hetero-junctions are most commonly created by forming a solution containing the two components, casting and then allowing the two phases to separate. The two components will self-assemble into an interpenetrating network connecting the two electrodes [5]. They are normally composed of a polymer based donor and fullerene based acceptor. The nonstructural morphology of bulk hetero-junctions tends to be difficult to control, but is critical to photovoltaic performance.

fter the capture of a photon, electrons move to the acceptor domains, then they are carried through the device and collected by one electrode, and holes move in the opposite direction and collected at the other side. If the dispersion of the two materials is too fine, it will result in poor charge transfer through the layer [6 and 7].

Most bulk hetero-junction cells use two components, although three-component cells have been also explored. The third component, a secondary p-type donor polymer, acts to absorb light in a different region of the solar spectrum. This in theory increases the amount of absorbed light. These ternary cells operate through one of three distinct mechanisms: charge transfer, energy transfer or parallel-linkage [8].

In charge transfers, both donors contribute directly to the generation of free charge carriers. Holes pass through only one donor domain before collection at the anode. In energy transfer, only one donor contributes to the production of holes. The second donor acts solely to absorb light, transferring extra energy to the first donor material. In parallel linkage, both donors produce excitons independently, which then migrate to their respective donor/acceptor interfaces and dissociate [8].

1.3 FACTORS LIMITING DEVICE EFFIENCY IN ORGANIC PHOTOVOLTAIC

The advancement of the power conversion efficiency of organic solar cells, reaching 10 % recently, in single-junction and tandem cells has been achieved by the development of new material and devices architecture, directed by an enhanced understanding of the operational mechanism. The real limit to organic photovoltaic cell power conversion efficiency may be a simple question, yet it is complex and it has to be analyzed and discussed in the smallest details [9].

In organic photovoltaic the devices cannot be used the same as semiconductors in inorganic photovoltaic devices, because the localized nature of the electronic state and the low dielectric permittivity cause photo-excited state to be confined to a small volume (few nm^3) in space and create a large (0,1- 1,0 eV) Coulobic barrier to dissociation into separate electrons and holes. In most organic photovoltaic devices, this is addressed by using a hetero-junction

of two different organic semiconductor with offset energy levels, the donor (D) and acceptor (A), that makes that D^+/A^- charge transfer state is more energetically favorable than exciting state of their D or A. Low mobility leads to poor collection efficiency but can be addressed by using thin layer with high absorbency or through improved materials [9]. The interplay between molecular structure, self-assembly, light absorption, band structure, material distribution and charge mobility is complex and makes it a fascinating and fruitful area of research, as evidenced by increasingly large number of studies published within the field each year [10].

The key factor that distinguishes organic solar cells from single-junction conventional photovoltaic devices in theoretical sense is the hetero-junction. Whilst research efforts are likely to deliver organic semiconductors with high enough mobility to enable collection across optically thick devices layer and high selective organic semiconductor-electrode contact, they are unlikely to eliminate the need for a hetero-junction. To incorporate the effect of the hetero-junction property, it is necessary to understand the mechanism of the charge separation [9].
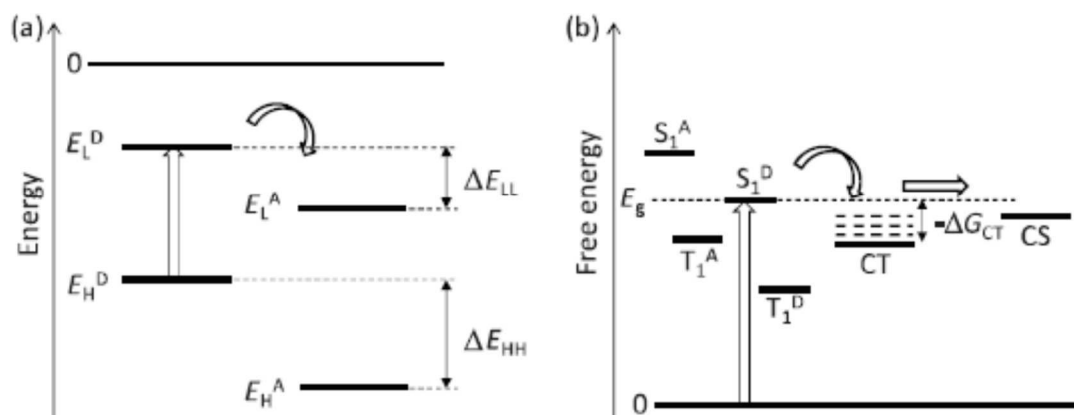

Figure 3 a) Energy levels involved in charge separation in a single-junction particle picture.
b) Energy levels involved in charge separation in state-diagram picture. In this diagram is assumed excitation of the donor to the singlet state. Excitation of the acceptor or excitation to a triplet state would be to equivalent processes, production the same D^+/A^- CT and CS states, although possibly with different kinetic.

Among the advantages of bulk hetero-junction photovoltaic, their potential to be fabricated easily via solution deposition and at low cost gives them a significant advantage over other solar technologies. The small molecule materials for use in photovoltaic research have been thoroughly studied.. The small molecule materials, which have advantages over more commonly used polymeric materials in terms of their ease of synthesis and purification; making them more affordable to produce on large scales [10, 11, and 12].

1.3.1 Basic efficiency relation in OPV

In the simplest, empirical approach, the solar cell is modeled as a current generator in parallel with a diode, generating two opposing currents when illuminated. There are added to deliver a net current density J at given potential difference between the terminals, V:

$$J = J_0\left(\exp(qV/nkT) - 1\right) - J_{SC} \tag{1}$$

where J_{SC} represents the short-circuit current density delivered by the light, J_0 is the saturation dark current of the diode, q is the elementary charge, k is the Boltzmann constant, T the temperature, and n the diode ideality factor. In conventional devices, J_0 relates to the ease of charge transport and injection over the p-n junction and mainly influence the open-circuit voltage V_{OC} while n relates to the mechanism of charge recombination and the fill factor, *FF* [9].

1.3.2 Practical efficiency limits

The question of limiting efficiency in OPV require highly ideal materials with properties that are the absorption spectrum, the exciton lifetime, the charge carrier mobility, or the required offset between energy levels to dissociate excitons into free charges. By the establishing empirical limit to the efficiency, it is not so much answer obtained that is relevant, but rather the question of which of the identified losses may be avoidable [9].

This led to development of new materials with small optical gaps, in order to increase photo-current and possibility open-circuit voltage. In the effort to design such polymers, attention was paid to the frontier orbital energy levels of donor and acceptor (for open-circuit voltage), the number of photon absorbed, and the driving force for charge transfer [9].

First publish quantitative design rules for donor in bulk-heterojunction solar cells using phenyl C_{61} butyric acid methyl ester (PCBM) as common acceptor [9]. These design rules are based on an empirical estimate of the open-circuit voltage (V_{oc}) in terms of energies of the HOMO of the donor (E^D_{HOMO}) and the LUMO of the acceptor (E^A_{LUMO}) thus:

$$V_{oc} = (1/q)\cdot\left(-\left|E^D_{HOMO}\right| + \left|E^A_{LUMO}\right|\right) - 0,3\,V \tag{2}$$

where 0,3 V is an empirical value, representing losses in transport to the electrodes [9].

The formula builds on previous studies which demonstrated that both E^D_{HOMO} and E^A_{LUMO} directly affect the V_{oc}, and holds provide that ohmic contact are realized with the active layer [9].

An energy difference $\Delta E_{LL} = 0,3$ eV between the LUMO of the donor and the LUMO of the acceptor is sufficient for efficiency charge separation. The energy difference between the two HOMO levels must fulfill the same criterion to prevent energy transfer rather than the desire electron transfer. By considering that photons are only absorbed by the polymer and not by the fullerene the limit to power conversion efficiency then only depends on the LUMO level of the donor. To obtain a practical limit to the efficiency assumed that the *EQE* (external quantum efficiency) of the solar cell for photon energies equal to or larger than the band gap

energy of the donor and the *FF* (fill factor) of the cell are both equal to 0,65. These number were chosen as representative of the best experimental system at the time based on these assumptions, the limit of single junction organic solar cells is 10% donor material with HOMO and LUMO equal 1,65 eV and 1,35 eV with band-gap 0,3 eV.. They do not represent fundamental limits, and have in fact been exceeded in several optimized cells ready [9].

1.4 THE PRINCIPLES OF MEASURING PHYSICAL AND OPTICAL VARIABLES

The solar cell is illuminated by a point of radiation source and current-voltage characteristic is measured.

Energy conversion efficiency of radiation to electrical energy is defined by the relationship in eq. 2.

$$\eta = \frac{P_{max}}{P_0} = \frac{U_{max} \cdot I_{max}}{P_0} = \frac{I_{sc} \cdot V_{oc} \cdot FF}{S \int_0^\infty M(\lambda) \cdot \frac{hc}{\lambda} d\lambda} \tag{3}$$

where P_0 is the power of the radiation incident on the cell surface S, P_{max} is the maximum power obtained from the article (which corresponds to the absolute value of the largest product of the voltage and current U_{max} and I_{max} – eq.3, I_{sc} (Short Circuit) is an electrical short circuit current (at zero voltage), V_{oc} (Open Circuit) is the open circuit voltage (at zero current) and *FF* is called filling factor (factor Field). The integral in equation (eq. 3) represents the total power of the incident radiation per unit area $M(\lambda)$ is the spectral density of the incident electromagnetic radiation (eq. 4) and a member of hc/λ represents the energy of one photon of wavelength λ.

The fill factor (Factor Field) FF is obvious from eq. 4.

$$FF = \frac{P_{max}}{I_{sc} \cdot U_{oc}} = \frac{|U_{max} \cdot I_{max}|}{I_{sc} \cdot U_{oc}} \tag{4}$$

Graphically it can be represented as a proportion of the area of a rectangle with sides U_{max} and I_{max} and rectangle with sides V_{oc} and I_{sc} in eq. (4). Due to the possibility to compare the efficacy produced by solar cells, it indicates efficiency when irradiated with spectral characteristics similar to that of sunlight for the perpendicular passage layer of the atmosphere (eq. 3). For these purposes are made so. Solar simulators AM1 (Air Mass 1), the integral radiant power is 760 W·m^{-2} (sometimes used value of 1000 W·m^{-2}, which the abbreviation AM1.5) [17].

1.5 ORGANIC MATERIALS FOR ORGANIC PHOTOVOLTAIC DEVICES

We are seeing organic materials in electronics for many years, which can be surprising because mostly polymers that we know are widely used as packaging materials, low molecular weight organic compounds are used to color.

Organic molecules contain double bonds. If the molecule will be alternating double and single bonds are talking about the known as conjugated system. This system able to lead excitation generated electric potential after their levels. With this phenomenon we are trying to take advantage of low molecular weight organic compounds with, in this particular case DPP, to prepare inexpensive and easy to use electric power source.

The biggest advantage in organic materials is the possibility to simple edits their properties as needed and creates new materials for a wide range of application possibilities [13].

The pigments come from the paint industry. They are small molecules bearing specific properties relevant to light absorption and charge generation. They are deposited in thin films from a solution (wet process). They can be soluble in various solvents. Pigments usually form polycrystalline thin films. This will possibly make them a competitive alternative to the various forms of silicon cells [14].

Among other materials the diketopyrrolopyrroles (DPP) have attracted the scientists as they represent a promising class of materials for several reasons:

- They can be processed easily using spin coating.

- Amounts of DPP materials are relatively small (100 nm thick films) and large scale production (chemistry) is easier than for inorganic materials (growth processes).

- They can be tuned chemically in order to adjust separately band gap, valance and conduction energies, charge transport, as well as solubility and several other structural properties [14].

1.5.1 DPP in molecular bulk-heterojunctions

Bulk heterojunction (BHJ) solar cells have been dominated by polymeric donor materials as they typically have better film-forming characteristics and film morphology than their small-molecule counterparts. Despite these advantages, the polymers suffer from synthetic reproducibility and difficult purification procedures, which hinder their commercial viability. Small-molecule materials, however, offer advantages over polymeric materials in terms of ease of synthesis and purification, which greatly improves fabrication reproducibility, as well as possessing a greater tendency to self-assemble into ordered domains, which leads to high charge carrier mobilities. These properties make small molecules a promising class of donor material for BHJ solar cell applications [15].

This progress is chiefly attributable to the introduction of the donor-acceptor hetero-junction that functions as a dissociation site for study the strongly bound photo-generated exciton. Further progress was realized in the polymer devices through using blends of the donor and acceptor materials. Phase separation during spin-coating leads to a bulk hetero-junction that removes the exciton diffusion bottleneck by creating an interpenetrating network of the donor and acceptor materials. Phase separation induced by elevating the substrate temperature inevitably leads to a significant roughening of the film surface and short-circuits devices [16].

EXPERIMENTAL PART

In the experimental part of this thesis, new DPP derivatives with different *N*-substitution and with phenyls or thienyls attached to the pyrrolopyrrole core are investigated in order to evaluate how such substitutions affect light absorption and performance in bulk hetero-junction solar cells. While the optical absorption and frontier orbital energy levels are mostly affected by the presence of phenyl or thienyl, the material´s solubility, thermal properties, film morphology, charge carrier mobility, and photovoltaic performance are altered significantly also by the *N*-substitutions due to differences in material properties arising from change in intra- and intermolecular interactions in the solid state [12].

First, solutions from the samples were prepared. The ability to dissolve and optical properties such as absorption and fluorescence were analyzed. Then thin layers were prepared. The layers were analyzed in order to determine the position of the absorption band and absorption edge, thickness of the layers, and overall morphology and occurrence of crystal phase. Based on the obtained optical properties and the ability to form good thin layer, two new derivatives were chosen to prepare solar cells and measure their photovoltaic properties. The findings are discussed according to the differences in their chemical structure.

2.1 MATERIALS

The goal of this work was to compare the effects of various substituents on the donor-acceptor pair in DPP. We focused on four new diketopyrroloprrole (DPP) molecules and one previously reported DPP(TBFu)$_2$ (sample 1), see Table 1. The new derivatives are DPP U115 (sample 2), DPP U116 (sample 3), DPP U117 (sample 4) and DPP U118 (sample 5). The already known DPP(TBFu)$_2$ has been previously reported as suitable for OPV applications and, therefore, was used here as a reference material.
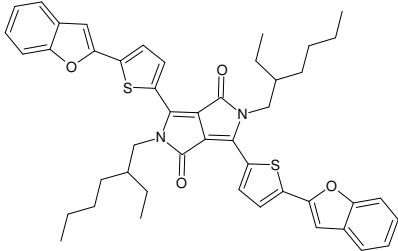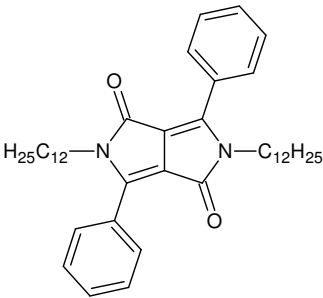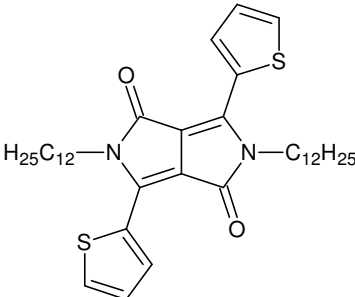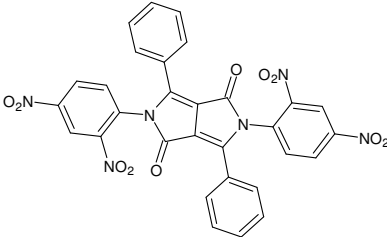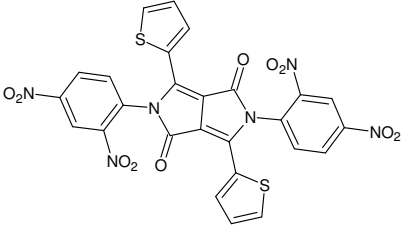
The differences between reference sample DPP(TBFu)$_2$ and the rest is in extension of the conjugated stystem by electron donating group (TBFu) and in *N*-substitution by ethylhexyl. The new materials have two main structural features:

1. The molecules contain either phenyl (DPP U115 and DPP U117) or thienyl (DPP U116 and DPP U118) connected to the diketopyrrolopyrrole core. This modification mainly influences energy of frontier molecular orbitals (FMO) (HOMO and LUMO) and geometry of the molecule.

2. *N*-substitution. A dodecyl group (DPP U115 and DPP U116) is used in order to provide necessary solubility and at the same time does not influence the HOMO and LUMO. Second substituent is dinitrophenyl (DPP U117 and DPP U118) – strong electron accepting group that is expected to largely influence the position and energy of the FMOs.

2.2 STRUCTURE AND BASIC PHYSICAL PROPERTIES

DPP(TBFu)$_2$ is a crystalline substance, it has a dark brown color, forms fine grains and with chloroform produces dark blue solution. Sample DPP U115 is deep orange in color and with chloroform forms yellow luminescent solution. Sample DPP U116 is red-brown color and creates deep orange phosphorescent solution with chloroform. Sample DPP U117 has similar color like DPP U115, is deep orange and creates deep orange solution. Sample DPP U118 is red colored and it´s solution with chloroform has red color. The appearance of the samples is showed in Figure 4. Samples DPP U115 and DPP U116 exhibit strong luminescence under UV light, as shown in Figure 5.

Table 1 Outline of samples with basic information

Molecular structure	info		
	Name	Sum. formula	mol. weight [g/mol]
	DPP(TBFu)2 (sample 1)	$C_{46}H_{48}N_2O_4S_2$ bisBenzFurTh Ph-bisEtHex-DPP (from COC) 1141/110	757,14
	DPP U115 (sample 2)	B/3056 JK.BDP.1409 2.01.03 $C_{42}H_{60}N_2O_2$	624,94
	DPP U116 (sample 3)	B/3007 JK.BDP.1308 06.01.02 $C_{38}H_{56}N_2O_2S_2$	636,99
	DPP U117 (sample 4)	D/1007 JD.DPP.12120 4.01.01COL $C_{30}H_{16}N_6O_{10}$	620,48
	DPP U118 (sample 5)	B/3005 JK.BDP.1309 06.01.02 $C_{26}H_{12}N_6O_{10}S_2$	632,54

Figure 4 Solutions of samples in chlorophorm. The samples are sorted incrementally from right to left.

Figure 5 Sample DPP U115 and DPP U116 under UV light in solid and liquid state.

.

2.3 OPTICAL PROPERTIES

Influence of the chemical structure on the optical characteristics is one of the key parameters of the materials used in OPV. To ascertain the influence of the chemical structure modification on the optical properties, we performed optical measurements of materials in solutions and in thin films.

2.3.1 Optical properties in solutions

From the characteristics of the solutions were determined the basic physical properties of the examined samples, which were compared in the following chapters.

2.3.1.1 Samples preparation

First, solutions were prepared from crystalline samples. As the solvent, chloroform from Lachner Company in p.a. purity was used. The sample DPP U117 and DPP U118 were poorly soluble and it was always necessary to use heating to 50 °C under a continuing stirring for 15 minutes for complete dissolution. Solutions of different concentrations of each sample were prepared. Summary of concentrations of each sample is given in Table 2.

Then, various concentrations were compared and molar absorption coefficient for each sample was determined.

Table 2 Concentrations of samples

Sample DPP(TBFu)$_2$	concentration [mol/ l]	Sample DPP U115	concentration [mol/ l]
1c5	$5,5 \cdot 10^{-6}$	2c5	$7,0 \cdot 10^{-5}$
1c6	$1,0 \cdot 10^{-5}$	2c6	$6,0 \cdot 10^{-5}$
1c7	$1,5 \cdot 10^{-5}$	2c7	$4,0 \cdot 10^{-5}$
1c8	$2,0 \cdot 10^{-5}$	2c8	$3,0 \cdot 10^{-5}$
1c9	$2,5 \cdot 10^{-5}$	2c9	$1,0 \cdot 10^{-5}$
1c10	$3,0 \cdot 10^{-5}$	$V = 4,0 \cdot 10^{-3}$	
1c11	$3,5 \cdot 10^{-5}$		
$V = 4,0 \cdot 10^{-3}$			

Sample DPP U116	concentration [mol/ l)]
3c5	$4,0 \cdot 10^{-5}$
3c6	$3,5 \cdot 10^{-5}$
3c7	$3,0 \cdot 10^{-5}$
3c8	$2,0 \cdot 10^{-5}$
3c9	$1,5 \cdot 10^{-5}$
V = $4,0 \cdot 10{-3}$	

Sample DPP U117	concentration [mol/ l)]
4c1	$1,0 \cdot 10^{-6}$
4c2	$2,0 \cdot 10^{-6}$
4c3	$3,0 \cdot 10^{-6}$
4c4	$4,0 \cdot 10^{-6}$
4c5	$5,0 \cdot 10^{-6}$
4c6	$6,0 \cdot 10^{-6}$
4c7	$7,0 \cdot 10^{-6}$
V = $4,0 \cdot 10{-3}$	

Sample DPP U118	concentration [mol/ l)]
5c5	$5,0 \cdot 10^{-6}$
5c6	$8,0 \cdot 10^{-6}$
5c7	$1,0 \cdot 10^{-5}$
5c8	$1,5 \cdot 10^{-5}$
5c9	$2,0 \cdot 10^{-5}$
5c10	$2,5 \cdot 10^{-5}$
V = $4,0 \cdot 10^{-3}$	

2.3.1.2 Absorption

Absorption was measured at laboratory temperature on the VARIAN Cary 50 Probe spectrophotometer. The measurements were performed against baseline from 800 nm to 200 nm and measurement speed was 600 nm/ min. For each material, the measurements were taken from the sample with the lowest levels concentration to the highest.

Three measurements were performed for the single concentration of each sample. These results were averaged and there are presented in Figure 6. For clarity, the curves were normalized to the maximal absorption.
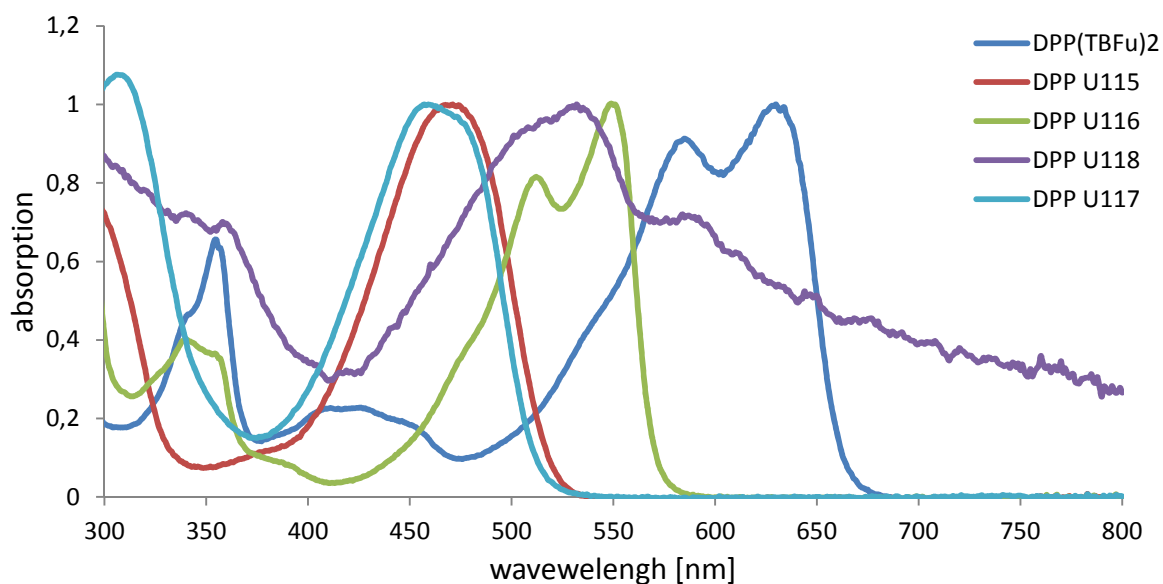

Figure 6 Absorption of the studied materials in chloroform.

The absorption curves in Figure 6 clearly shows how the substituent groups affect the energy of HOMO and LUMO levels, which results in a shift of the absorption peaks.

DPP U115 with phenyl groups occur to have the absorption at shorter wavelengths than DPP U116 that contains thienyl and thus has larger HOMO – LUMO difference. This behavior can be explained by shortening of the effective conjugation. The phenyls can relatively easily rotate and thus the conjugation is reduced. On the contrary, the thienyl rotation is restricted and the DPP U116 has more planar conformation with longer effective conjugation and smaller FMO energy difference. The thienyl groups thus represents better unit in order to provide better match with Solar radiation and thus improve the photovoltaic properties of organic solar cells.

DPP U117 is very poorly soluble and therefore the absorption curve is noisy. There is absorption of both the solubilized molecules and solid undissolved particles. The spectrum contains also the light scattering at the longer wavelength part of the spectra. The obtained absorption curves shows similar behavior to the dodecyl counterparts described above. The thienly group containing DPP U118 has bathochromically shifted absorption compared to the phenyl substituted DPP U117. The slight hypsochromic shift induced by the dinitroaryl group compared to the dodecyl is probably caused by even higher rotation of the phenyl and thienyl due to stronger steric hindrance.
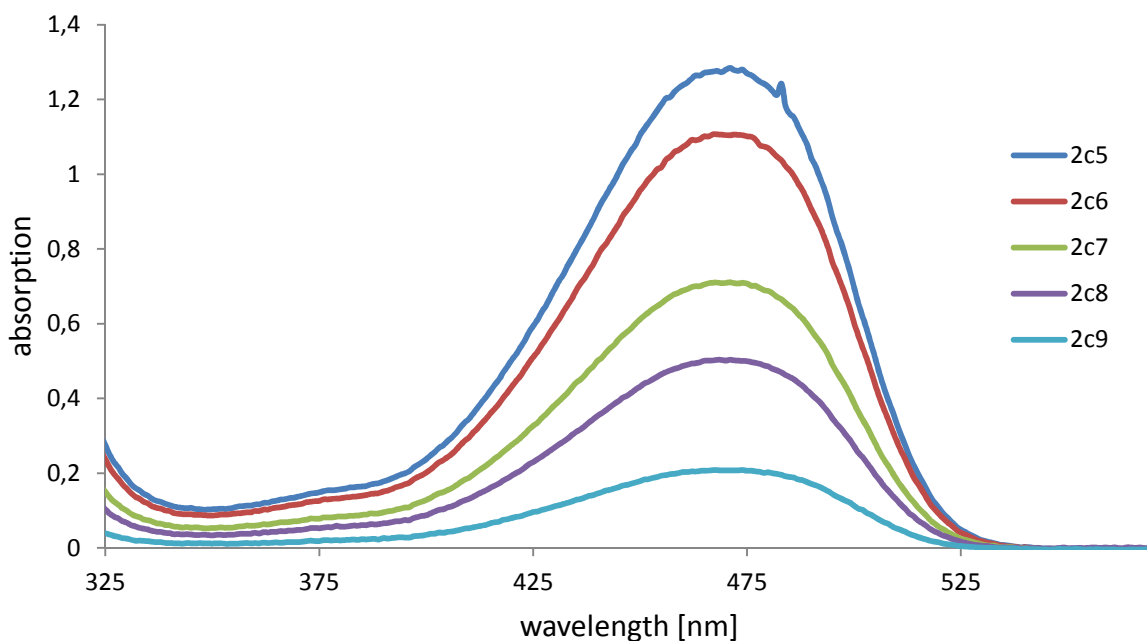
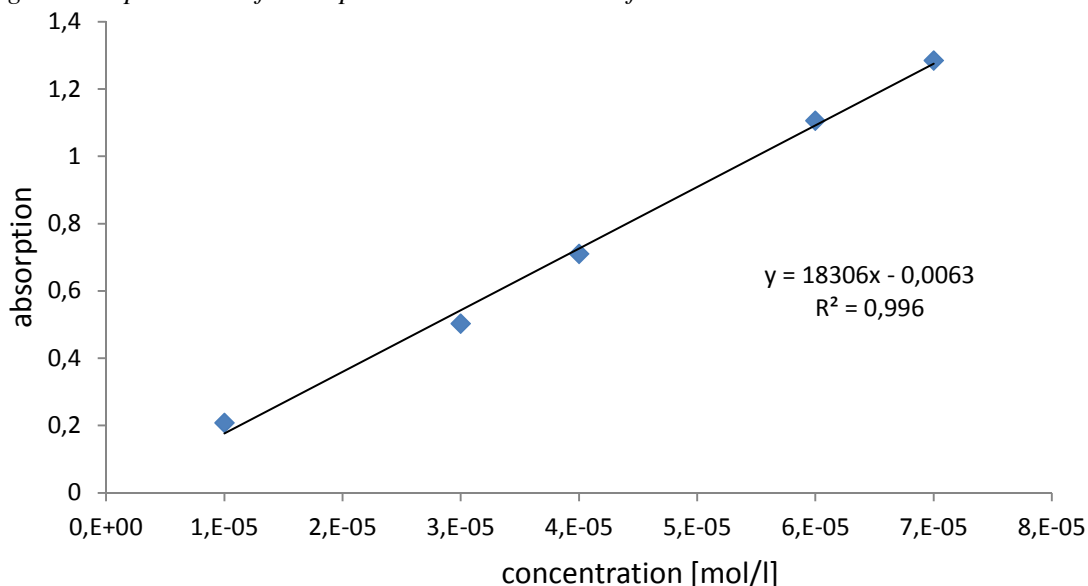*Figure 7 Dependence of absorption on concentration of the DPP U115.*

Figure 8 Plot of absorption at 472 nm on concentration used for molar absorption coefficient determination for DPP U115.

The figure 7 and 8 show the absorption of the samples for various concentration. The molar absorption coefficient was determined from the Lambert-Beer law (eq. 5) as a slope of the absoprtion on concentraion.

$$A = \varepsilon \cdot c \cdot l, \tag{5}$$

where A is absorpiton, ε is molar absorption coefficient and l is cuvettes lengh.

The results of the optical characterization is summarized in Table 3. The sample containing thienyl (DPP U116) has higher molar absorption coefficient than DPP U115 with phenyl. The thienyl containing DPP U117 which has *N*-substituted dinitrophenyl has higher molar absorption coefficient than its phenyl containing analog DPP U118. This is probably

caused by error in the molar absorption coefficient analysis due to its poor solubility. Samples DPP U117 and DPP U118 have molar absorption coefficients higher than the alternatives with an *N*-substituted aliphatic (dodecyl) side-chain.

hese observations are in accordance with the position of the absorption band discussed above. The thienyl provides more planar structures and therefore the absorption coefficients are higher. The dinitrophenyl group as a strong electron withdrawing group increases the electron deficiency of the pyrrolopyrrole core and thus leads to stronger internal charge transfer.

Table 3 results of the maximum absorbance, molar absorption edges and mol. abs. coefficient

Sample	Max. absorption [nm]	Absorption edge [nm]	Mol. absorption coefficient [l/mol·cm]
DPP(TBFu)$_2$	629	660	(52459 ± 0,02)
DPP U115	457	513	(18306 ± 0,01)
DPP U116	549	568	(28366 ± 0,17)
DPP U117	531	567	(20791 ± 0,01)
DPP U118	459	513	(62260 ± 0,12)

2.3.1.3 Fluorescence spectroscopy

To evaluate the presence and properties of fluorescence, a FLUOROLOG was used. The settings have been chosen with regard to the fluorescence intensity of one million, at which the accuracy of the instrument is the best. Results of emission and excitation are shown in Figures 9 to 14 together with the absorbance for each sample separately. The obtained fluorescence data are summarized in Table 4.

We have found that all of the derivatives exhibit fluorescence. The intensity and position were dependent on the chemical structure. The dodecyl *N*-substituted derivatives had strong fluorescence visible by naked eye under UV lamp irradiation, see Figure 4. The thiophene containing derivatives (DPP U116 and DPP U118) exhibit fluorescence with relatively small Stokes shift compared to the phenyl substituted derivatives. This corresponds to the higher rigidity and resulting planarity observed in the absorption spectra. Correspondingly, the phenyl containing derivatives exhibited larger Stokes shift due to increased phenyl rotation and flexibility.
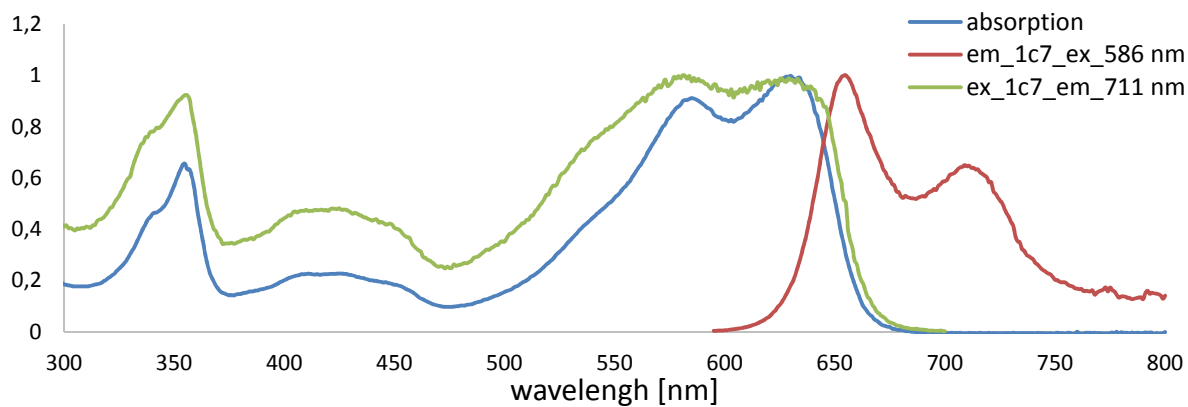
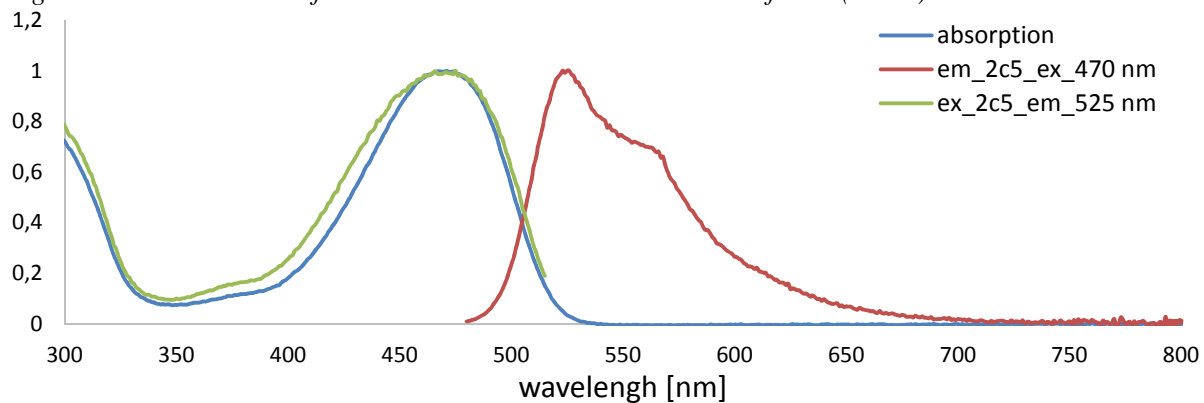*Figure 9 Absorbance and fluorescence emission and excitation of DPP(TBFu)2.*

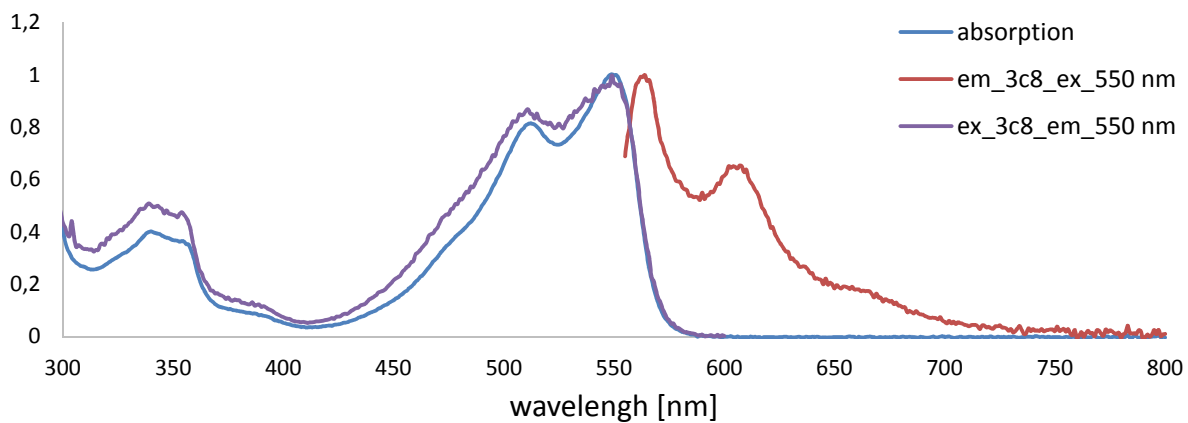*Figure 10 Absorbance and fluorescence emission and excitation of DPP U115.*

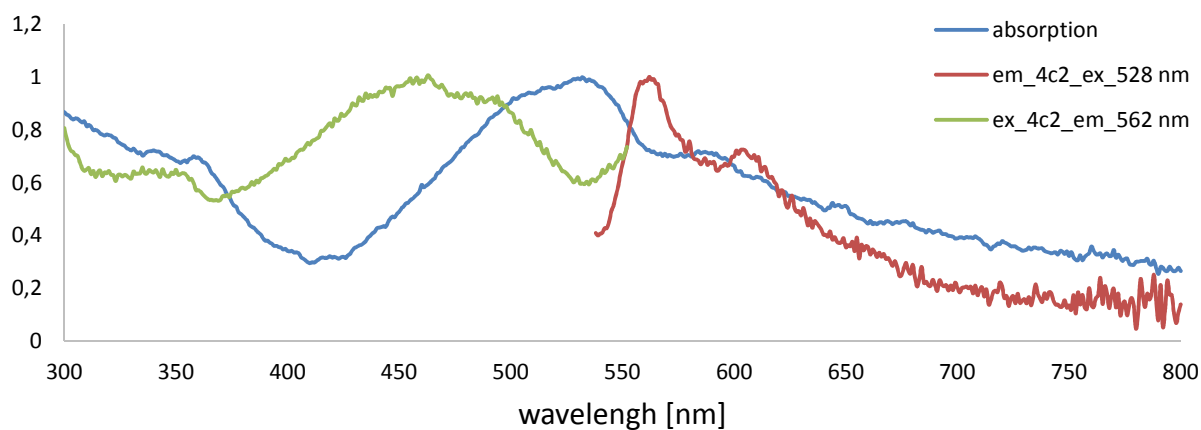*Figure 11 Absorbance and fluorescence emission and excitation of DPP U116.*

25

Figure 12 Absorbance and fluorescence emission and excitation of DPP U117.
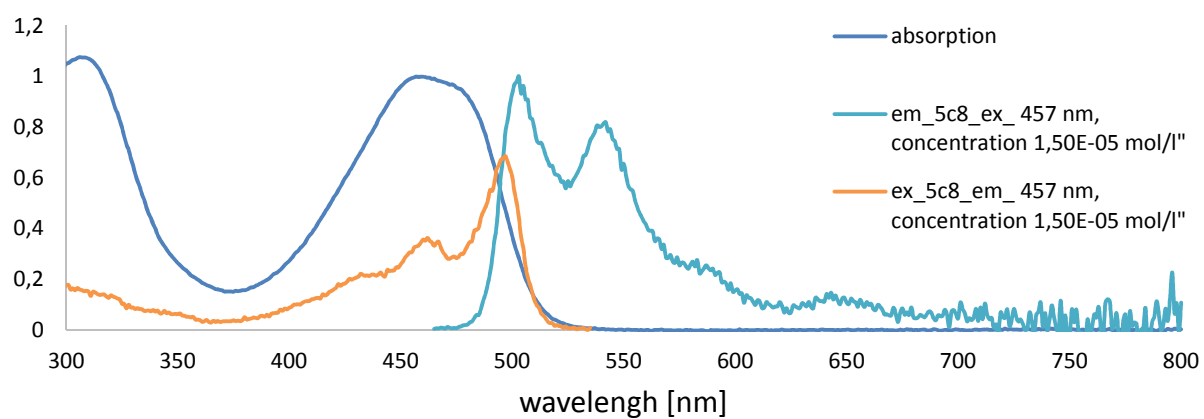

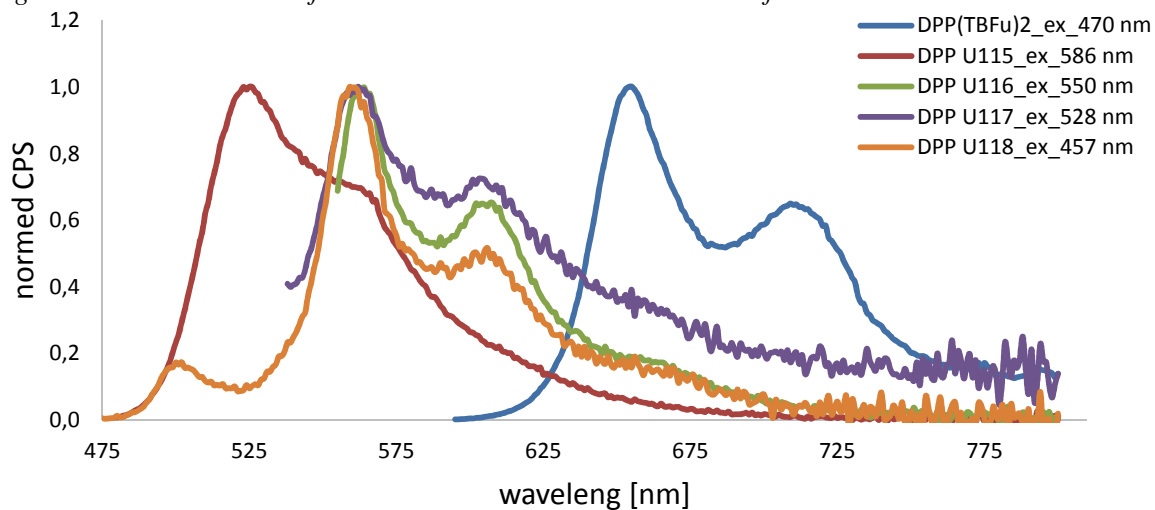*Figure 13 Absorbance and fluorescence emission and excitation of DPP U118.*

Figure 14 Normalized fluorescence of the DPP derivatives under study.

Table 4 Results of max. emission and Stokes shift

Sample	Max.emission [nm]	Stokes shift [nm]	Stokes shift [cm^{-1}]
DPP(TBFu)$_2$	655	25	$2{,}5 \cdot 10^{-6}$
DPP U115	457	68	$6{,}8 \cdot 10^{-6}$
DPP U116	549	15	$1{,}5 \cdot 10^{-6}$
DPP U117	562	31	$3{,}1 \cdot 10^{-6}$
DPP U118	503	44	$4{,}4 \cdot 10^{-6}$

2.3.1.4 Discussion

The optical characterization of the DPP derivatives revealed, that the presence of thienyl or phenyl group mainly governs the planarity and rotation flexibility and thus the thienyl groups lead to bathochromic absorption compared to the phenyls. The *N*-substitution does not influence the optical band-gap a lot.

This behavior was confirmed by the fluorescence spectroscopy: The thiophene containing derivatives (DPP U116 and DPP U118) exhibit fluorescence with relatively small Stokes shift due to the higher rigidity induced by the thienyl. Furthermore, the dodecyl *N*-substituted derivatives exhibited strong fluorescence visible by naked eye under UV lamp irradiation.

During these experiments, we also found out that solubility of the dinitrophenyl *N*-substituted derivatives is not good enough to use them to form thin films.

2.3.2 THIN LAYERS

In order to produce solar cells, thin layers have to be first formed. Therefore in this section we report on preparation and optical properties of thin films. Furthermore, we performed temperature annealing in order to explore the possible changes in the film structure during the thermal treatment.

2.3.2.1 Experimental

The thin film was prepared on a glass substrate on which the sample solution is then applied. The substrates were first cleaned in an ultrasonic bath. The substrates were first put in distilled water with STAR 50 surfactant and left in the ultrasonic bath for 15 minutes. Then the glass were left for 30 minutes in MilliQ water and then cleaned for 30 minutes in MilliQ water in the ultrasonic bath. Finally, the glass was rinsed with acetone and cleaned for further 15 minutes in an acetone in the ultrasonic bath.

The thin films were prepared using spin coating technique. Thin films were deposited initially at a speed of 3000 rpm, but because of poor quality of the resulting layers, the rate was decreased. All the reported results in this thesis are from thin films formed at the speed of 1500 rpm.

We have also investigated the influence of temperature on the thin films. Measurements were performed at laboratory temperature, 60 °C, 80 ° C, 100 °C, 120 °C and 140 °C.

2.3.2.2 Microphotography

The qualities of the prepared thin films were analyzed with the help of optical microscopy. A Nikon Eclipse E200 microscope with additional camera NIKON D5000 was used. Zoom was set at 20 times. Each photo has a normal version and a version with polarizing filter.
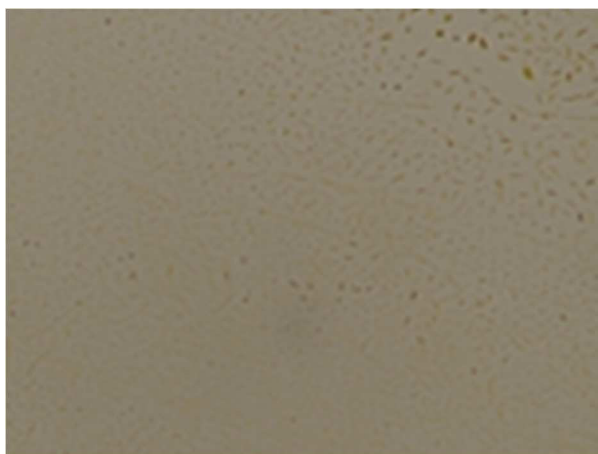
The following Figures 15 to 24 show the surfaces of thin layers at various temperatures, as evidence of the influence of temperature on the crystalline nature of the individual samples.
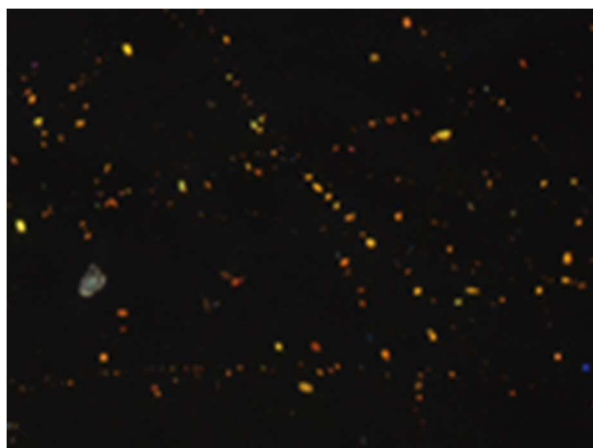
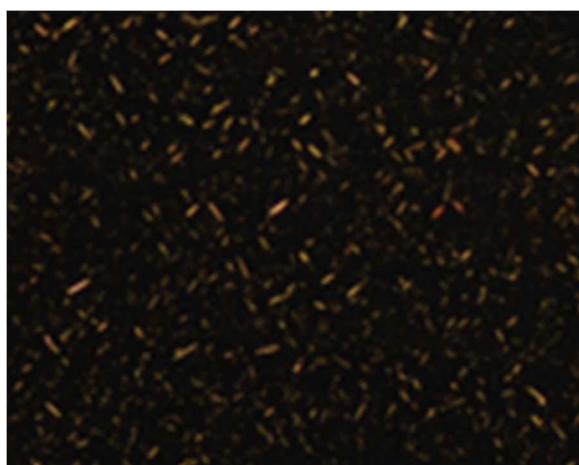*Figure 15 DPP(TBFu)2 at lab. temperature*

Figure 16 DPP(TBFu)2 at 140 °C

Figure 17 DPP U115 at lab. temperature

Figure 18 DPP U115 at 140 °C

Figure 19 DPP U116 at lab. temperature
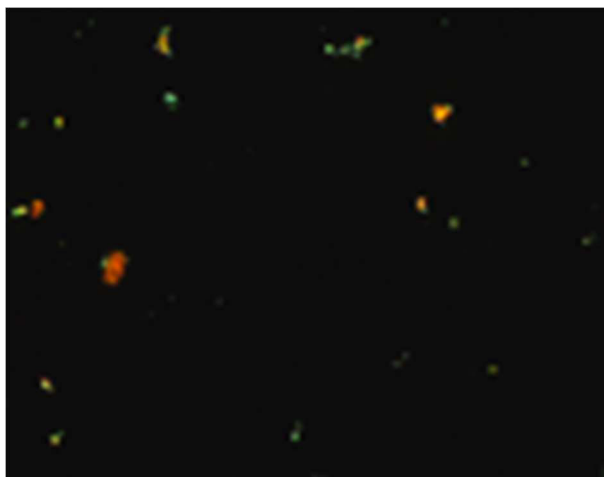

Figure 20 DPP U116 at 140 °C
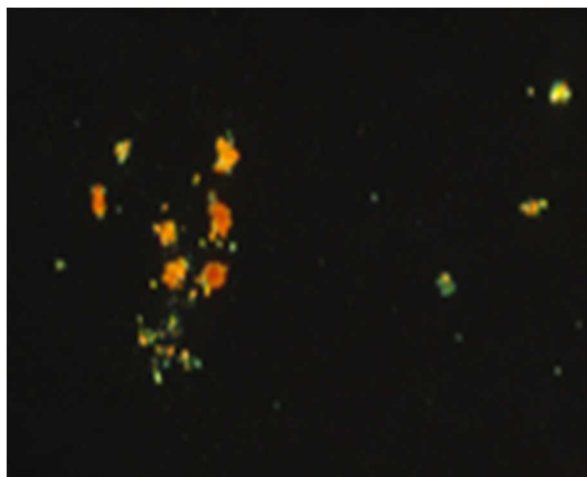
Figure 21 DPP U117 at lab. temperature
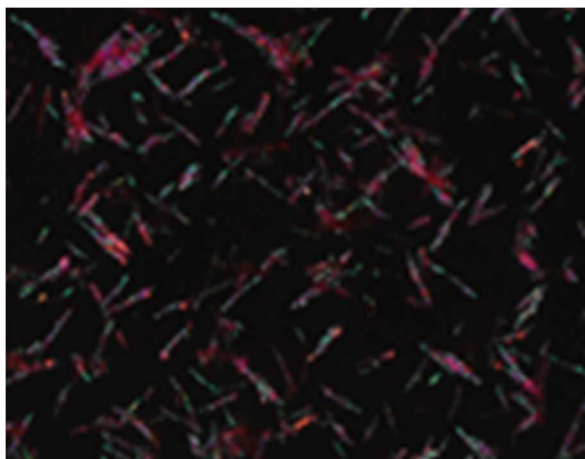

Figure 22 DPP U117 at 140 °C

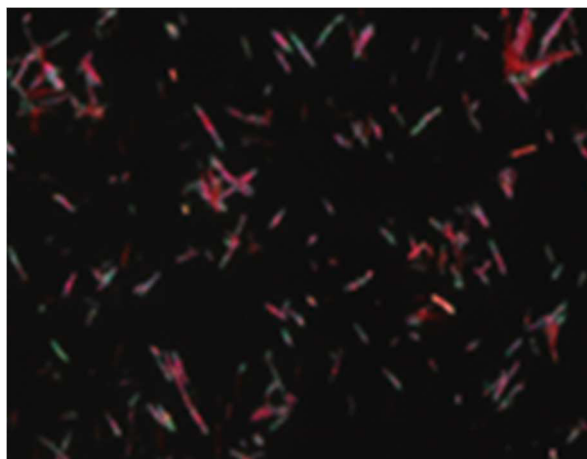*Figure 23 DPP U118 at lab. temperature*

Figure 24 DPP U118 at 140 °C

There was no substantial change observed in the thin films of the DPP(TBFu)$_2$ derivative. A small crystal growth of the DPP U115 due to increased temperature was observed. The DPP U116 exhibited significantly increased crystalinity already at 80 °C. Due to the poor solubility of the DPP U117, the as cast films already contained crystals and there was a noticeable increase of the amount and size f the crystals during annealing. Similarly, the thin films of DPP U118 contained crystals from the beginning (short elongated needles), but the annealing did not have any significant effect.

The presence and shape of crystals are closely related to the geometry and thus to the planarity of the molecules. The more planar molecules has higher tendency to have stronger π-π stacking, and the molecule has higher ability to form crystals. Such behavior was observed for thienyl containing derivatives DPP U116 and DPP U118.

2.3.2.3 Profilometry

The thickness of the prepared films was analyzed by mechanical profilometer DEKTAKXT from Bruker. The results are shown in Table 5. The thickness was obtained as a difference between the thin layer and the glass substrate in the scratched area. The resulting

value was obtained as the average of several measurements on different places of three scratches for each sample.

Table 5 Thickness of the thin film prepared form the studied DPP materials.

Sample	Thickness [nm]
DPP(TBFu)$_2$	(16 ± 4)
DPP U115	(6 ± 2)
DPP U116	(42± 3)
DPP U117	*
DPP U118	(105 ± 6)

Unfortunately it was not possible to measure the thickness of DPP U117, because the crystals were not dissolved and a homogeneous thin layer was not formed. The crystals were irregularly distributed over the sample.

The results show that DPP (TBFu)$_2$, DPP U115 and DPP U116 and DPP U118 created relatively homogeneous thin films. The DPP U117 was not possible to measure. The ability to create thin layers is closely related to the solubility of the material. While DPP (TBFu)$_2$, DPP U115 and U116 DPP showed no signs of problems with dissolving, DPP U117 and U118 DPP had to be always heated and even so they did not completely dissolved that resulted in a fragmented thin layer.

2.3.2.4 Absorption

In order to evaluate the influence of the chemical structure modification on the photovoltaic properties, optical properties of the thin films were also analyzed for different annealing temperature. Three measurements were performed for the single sample for each temperature. The normalized absorption spectra of the DPP(TBFu)$_2$, DPP U115 and DPP U118 are presented in Figure 25. The DPP U117 and DPP U118 were not used due to their poor film forming properties. Absorbance was measured at room temperature on the VARIAN Cary 50 Probe against baseline correction from 800 nm to 200 nm and the measurement speed was 600 nm/ min.
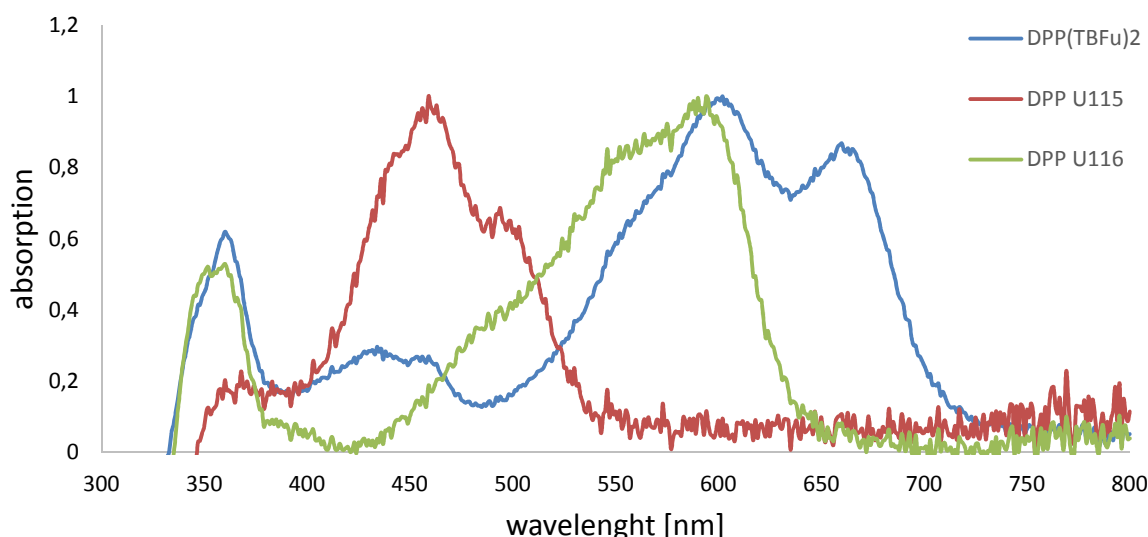
Figure 25 Plot of influence Absorbance on wavelength at lab. temperature.

Here it is seen that for thin films occurred to shift to higher wavelengths than for solutions in the sample DPP U116 and DPP(TBFu)2. Sample DPP U115 did not change max. absorption. Samples DPP U117 and DPP U118 were discarded because of poor ability to form thin layer. Results max. abs. and the absorption edge are shown in Table 6.

Table 6 Result of max abs. and abs. edge

Sample	Max. absorption [nm]	Absorption edge [nm]
DPP(TBFu)$_2$	602	660
DPP U115	459	513
DPP U116	594	630
DPP U117	*	*
DPP U118	*	*

2.3.2.5 Temperature annealing

Ability of crystallinity at increasing temperature is important for the charge transfer. The more crystallinity is greater, the easier is the ability to conduct charge, therefore the samples were tempered.
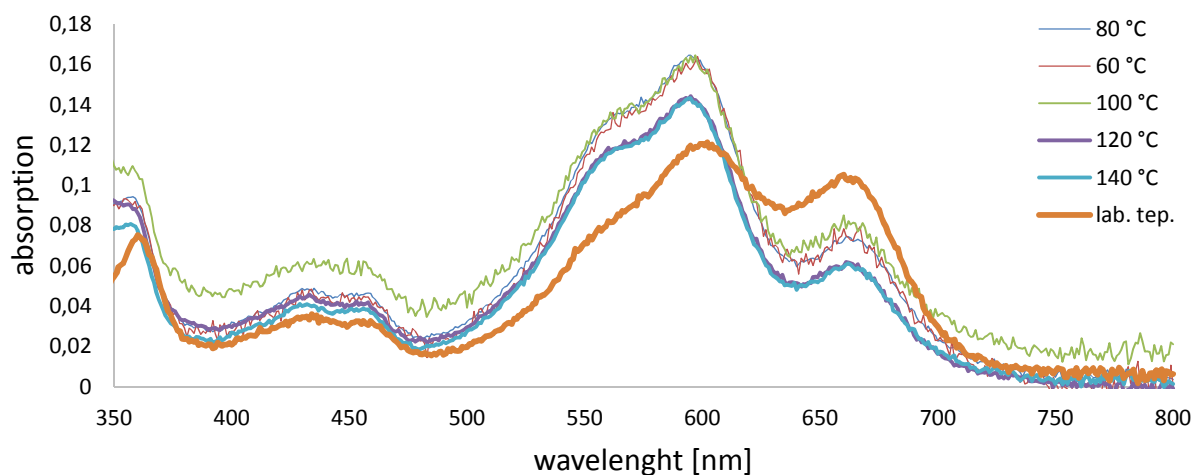
Figure 26 Plot of annealing in sample DPP(TBFu)2.

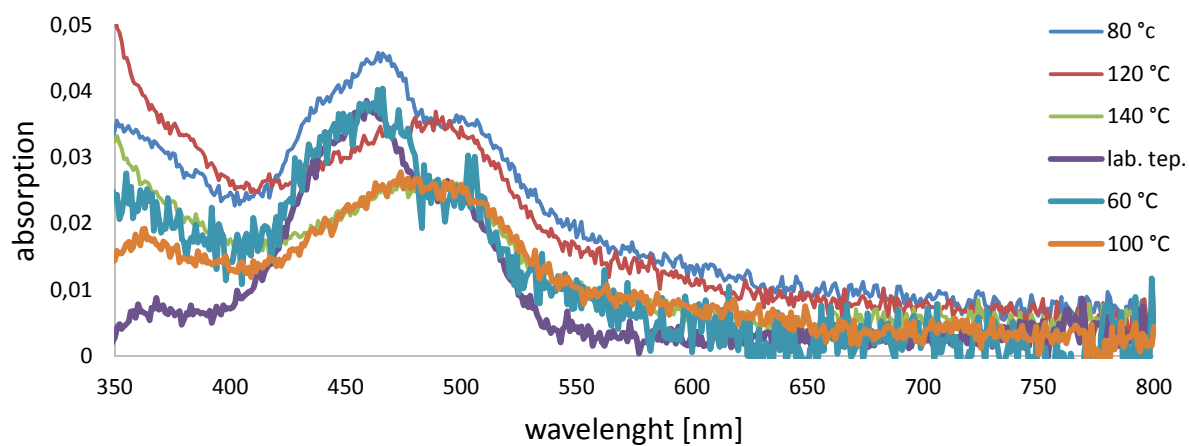The highest absorption achieved sample DPP (TBFu)2 at 80 ° C.

Figure 27 Plot of annealing in sample DPP U115.

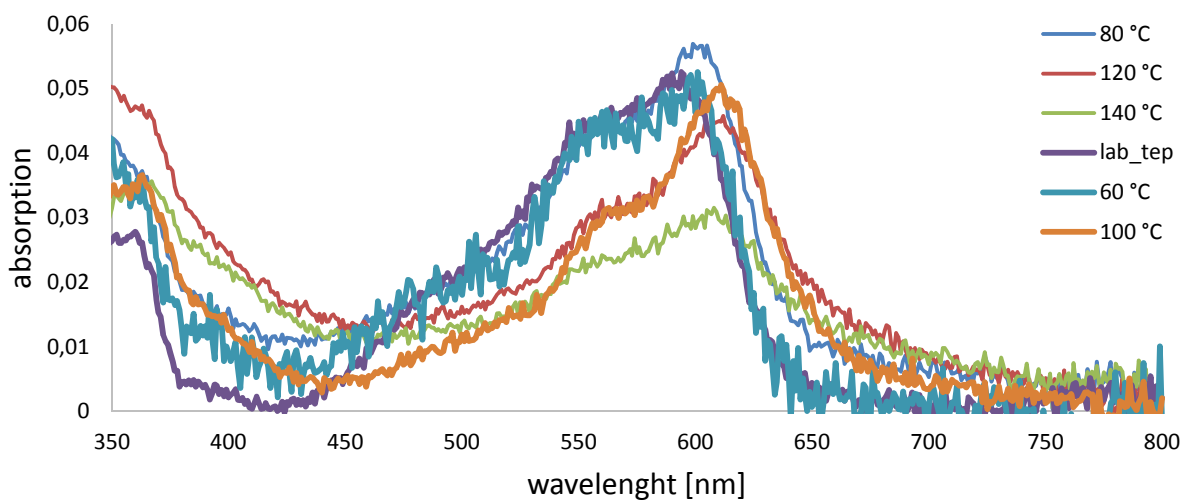The highest absorption achieved sample DPP U115 at 80 ° C.

Figure 28 Plot of annealing in sample DPP U116.

The highest absorption achieved sample DPP U116 at 100 ° C.

Samples DPP (TBFu)2 and DPP 115 have the highest absorption after tempering at 80 °C. Sample DPP U116 has the highest absorption at 100 °C, which is likely due to the presence of thiophene.

Samples DPP U117 and the DPP U118 because of poor solubility sufficiently didn´t dissolve and so the results did not show any absorption depending on the annealing.

2.3.2.6 Flour spectrophotometry

They were used same samples like for absorption, for flour spectrophotometry measurement.
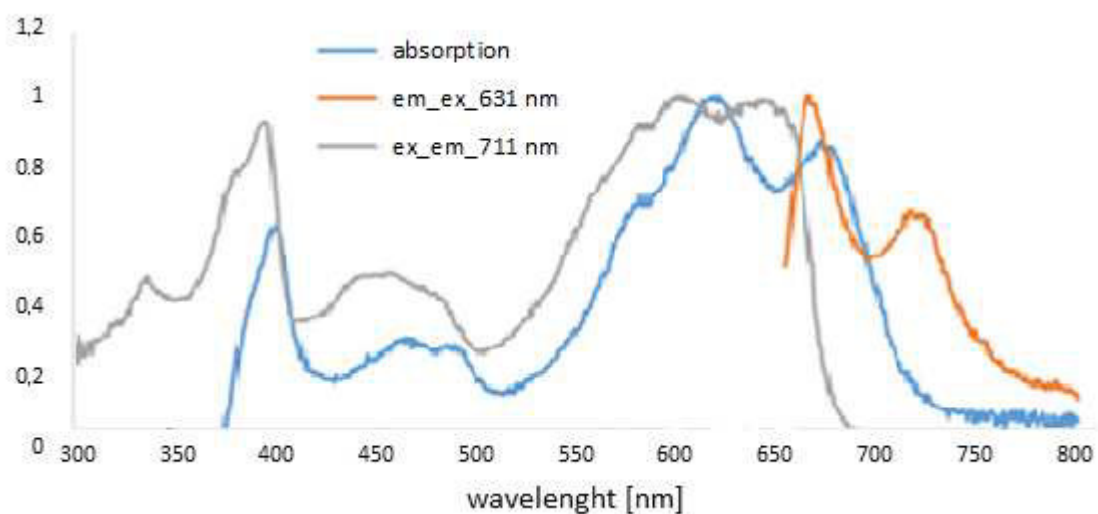

Figure 29 Plot of comparing absorbance, emission and excitation in the sample DPP(TBFu).

The emission spectrum of thin layer corresponds to emission spectrum of solutions. There was no significant shift.
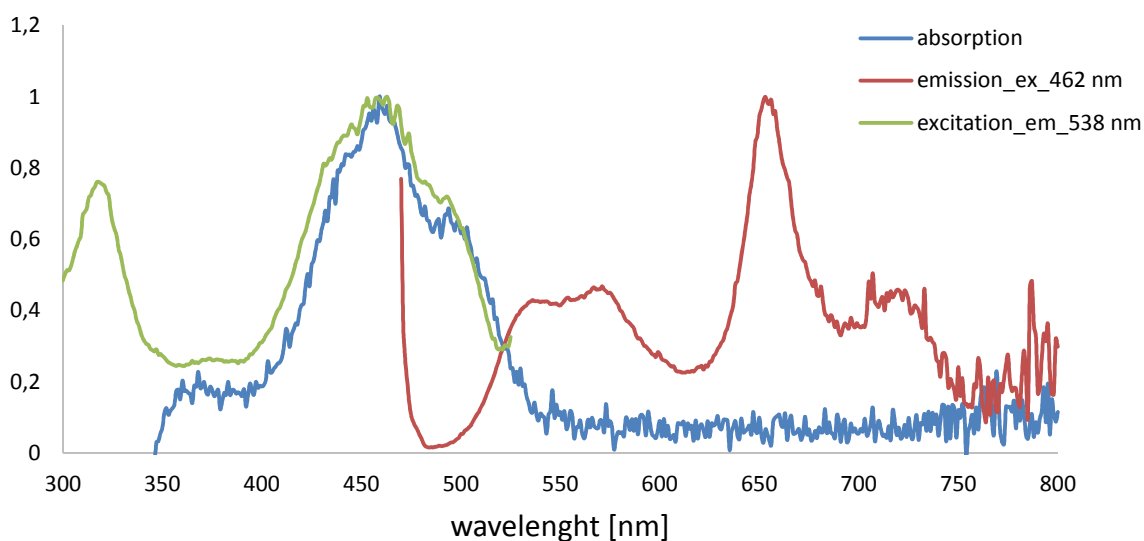

Figure 30 Plot of comparing absorbance, emission and excitation in the sample DPP U115.

Emission spectrum of thin layers in sample DPP U115 was different as compared to the solution. There was a shift to higher wavelengths and change of the character the emission curve.
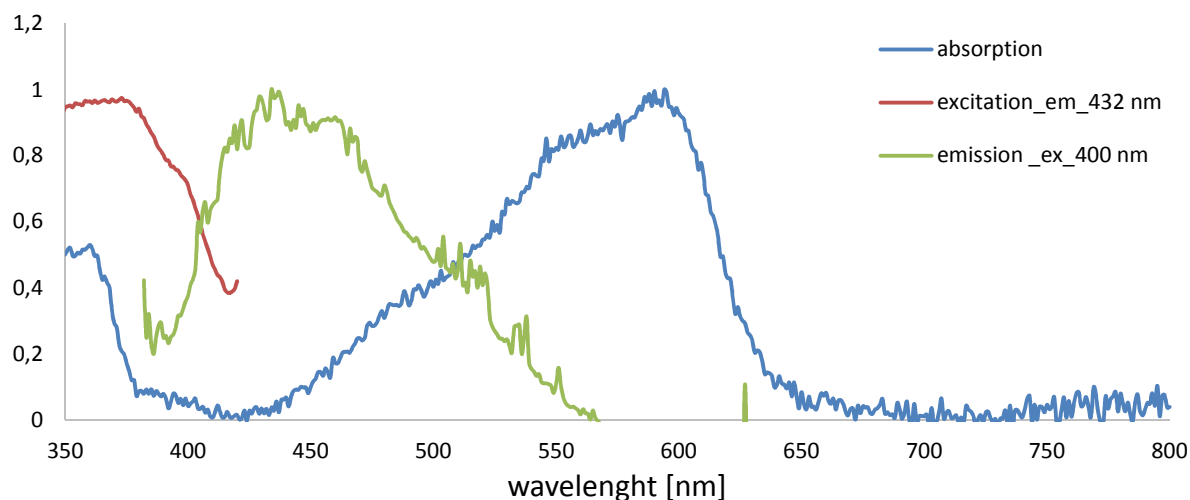
Figure 31 Plot of comparing absorbance, emission and excitation in the sample DPP U116.

Emission spectrum of thin films at sample DPP U116 is completely different than in solution. There has been a significant shift to lower wavelengths and a change of the character of the emission curve.
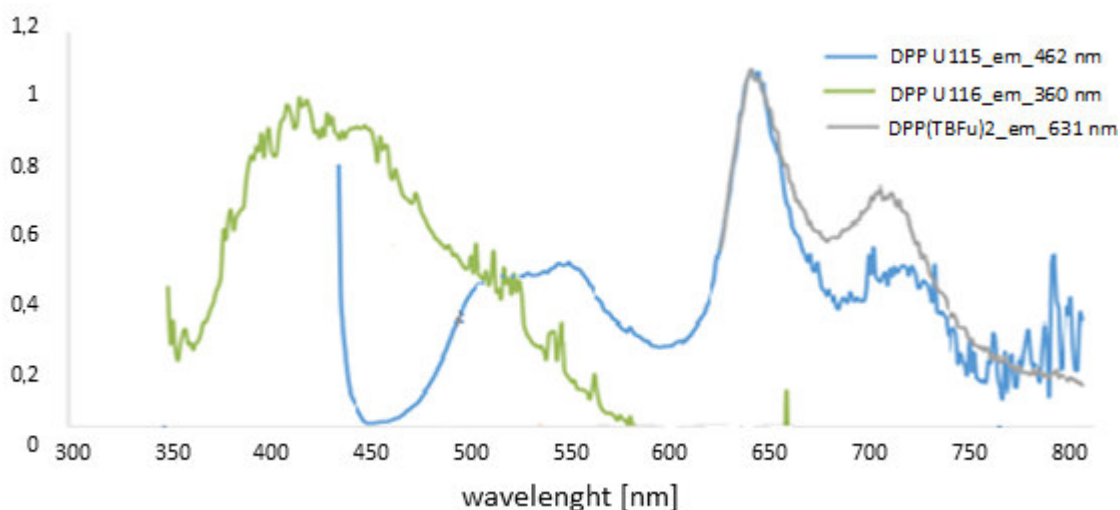
Figure 32 Plot oft dependence wavelength to normed emission.

Emission spectra of thin layer were different from emission spectra of solutions. It was probably due to the increase crystallinity at thin layer against solution. In sample DPP U115, which contains phenyl, there was a shift to larger wavelengths. In sample DPP U116 that contains thiophene, there was a significant shift in the emission spectra to lower wavelengths. Results of max. emissions and Stokes shift are shown in Table 7.

Table 7 Results of max. emission and Stokes shift

Sample	Max. emission [nm]	Stokes shift [nm]	Stokes shift [cm^{-1}]
DPP(TBFu)$_2$	655	53	$5,3 \cdot 10^{-6}$
DPP U115	653	194	$1,94 \cdot 10^{-5}$
DPP U116	485	109	$1,09 \cdot 10^{-5}$
DPP U117	*	*	*
DPP U118	*	*	*

2.3.2.7 Discussion

This implies that the dodecyl group prevent close packing.

A description of the behavior of pigments in thin layers compared to solutions is main for the proper application of OPV. It was observed inability of samples DPP U117 and U118 DPP form thin layers due to poor solubility.

From thermal annealing was revealed that the highest absorption in samples DPP(TBFu)$_2$ and DPP U115 were reported after tempering to 80 °C and for the sample DPP U116 at 100 °C, which is associated with the increase of the crystallinity with increasing temperatures.

Further, samples DPP(TBFu)$_2$, DPP U115 and DPP U116 were studied at the differences of optical properties of thin layers compared to solutions. Absorption was for samples DPP(TBFu)$_2$ and DPP U116 shifted to higher wavelengths. Emission spectra were for sample DPP U115 shifted to higher wavelengths and sample DPP U116 to lower wavelengths.

2.4 PHOTOVOLTAIC PROPERTIES

Based on the previous results, samples DPP(TBFu)$_2$, DPP U115 and DPP U116 were selected to investigate their photovoltaic properties.

2.4.1 Experimental

The production of photovoltaic cells that has a maximum efficiency of about 4% can be divided into 10 steps. First was to purify the underlying glass substrate with transparent electrodes. Cleaning was carried out in the same solution as used for preparation of thin film of the material to be deposited. PEDOT:PSS, purchased from Ossila, was then coated on the cleaned substrate. All work was carried out in an inert atmosphere (N$_2$), and in the laboratory with controlled particle content in the air (cleanroom). The PEDOT:PSS layer was applied using the dynamic spin coating at speed 5000 rpm for 40 seconds and the volume of the coating solution was 0.06 ml. Cathode strip was cleaned after that. Then, thermal annealing was performed. The sample was maintained at 150 °C for 5 minutes.

After cooling the sample, the DPP layer was applied. DPP(TBFu)$_2$ was mixed before application with PCBM in the ratio 1:0.6. A thin layer from 0.05 ml was applied again with dynamic spin coating at a speed of 2500 rpm for 30 seconds. Cathode strip was then cleaned.

The next step was deposition of electrodes. The substrate was placed on the shadow mask by the active layer downward and then the electrodes (aluminium) were deposited using vacuum evaporation.

One of the last steps is encapsulation which protects the thin layer from mechanical damage but mainly from exposure to oxygen and water vapor. First, a small amount of special epoxide is applied on the substrate. Then, a cover-slip was attached using tweezers on top and gently pressed so as epoxy covered the whole surface of glass. Subsequently, to cure the epoxide under UV light (~ 380 nm) the samples were exposed for 30 minutes. Then, the substrate can be removed from the glove box.

The encapsulated substrate was subsequently cleaned and fitted with contacts attached to the active side.

2.4.2 Reference DPP

Preparing a photovoltaic cell from the reference sample we tested methodology and procedure.
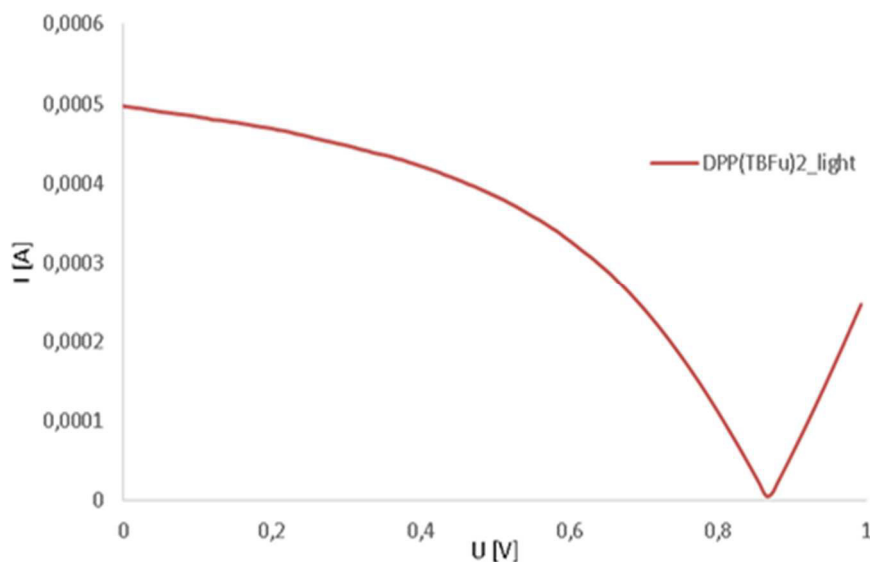

Figure 33 Plot of photocurrent DPP(TBFu)2

Table 8 Results of efficiency DPP(TBFu)2

Sample	J_{sc} [mA/cm^2]	V_{oc} [mV]	FF [%]	η [%]
DPP(TBFu)$_2$_light	8,26	866,63	46,10	3,30

The obtained efficiency of DPP(TBFu)$_2$ is about 4 %. The efficiency of our photovoltaic cell was 3,27 % and 3,30 % in a light mode. This indicates that the optimization and preparation of DPP(TBFu)$_2$ has been successful and the preparation and characterization methods were mastered. Results are shown in Table 8.

2.4.3 Photovoltaic performance of new DPP

Preparation of photovoltaic cells from DPP U115 and DPP U116 proceeded the same way as the preparation of the reference sample DPP(TBFu)$_2$.

In order to find the best conditions for the optimal performance of the sollar cells, concentration series were prepared with varying proportions of PCBM and DPP. The differences in their photovoltaic characteristics were then measured. Overview of the concentrations can be found in the Table 9.

Table 9 Overview concentrations PCBM for DPP U115

Sample	Volume of DPP [ml]	Volume of PCBM [mg]	Proportion
A	0,5	1,67	3:1
B	0,5	3,33	3:2
C	0,5	5	1:1
D	0,5	7,5	2:3
E	0,5	15	1:3
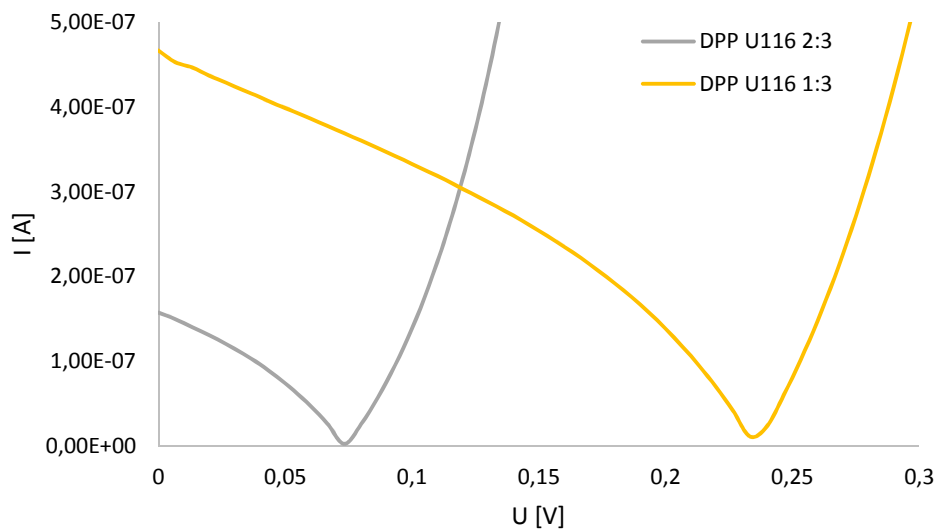
Figure 34 Plot of photocurrent DPP U115

Table 10 Results of efficiency DPP U115

Sample	J_{sc} [mA/cm^2]	V_{oc} [mV]	FF [%]	η [%]
DPP U115_D	$2,62 \cdot 10^{-3}$	73,78	33,16	$6,36 \cdot 10^{-5}$
DPP U115_E	$7,74 \cdot 10^{-3}$	234,99	34,92	$3,36 \cdot 10^{-4}$

The optimum concentration at which the highest efficiency of DPP U115 was measured was 1:3 (DPP:PCBM), see Table 11. Photocurrent of samples with concentrations A, B and C was under the resolution of the measurement device. Results are shown in Table 10.

Table 11 Overview concentrations PCBM for DPP U116

| Sample	Volume of DPP [ml]	Volume of PCBM [mg]	Proportion
A	0,3	1	3:1
B	0,3	2	3:2
C	0,3	3	1:1
D	0,3	4,5	2:3
E	0,3	9	1:3
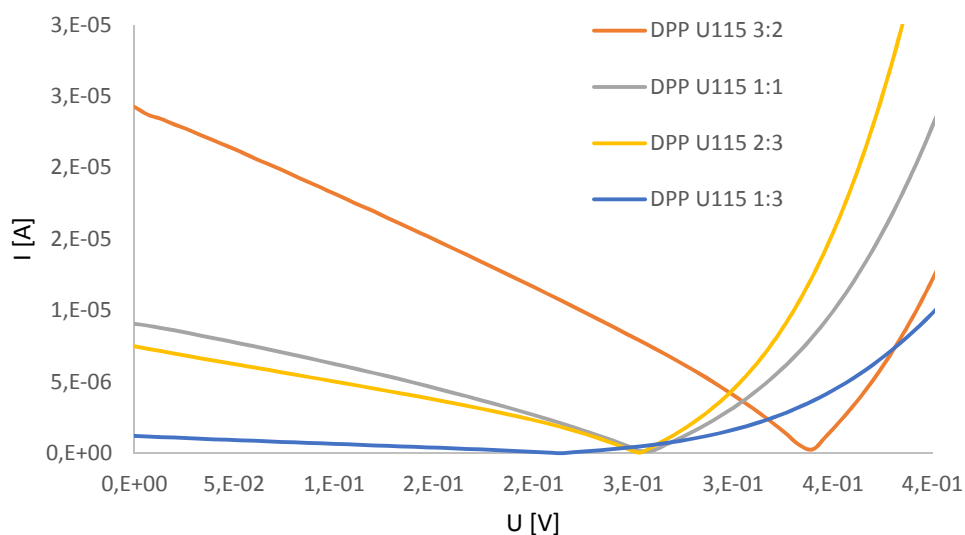
Figure 35 Plot of photocurrent DPP U116

Table 12 Results of efficiency DPP U116

Sample	J_{sc} [mA/cm^2]	V_{oc} [mV]	FF [%]	η [%]
DPP U116_B	0,40	336,18	28,81	0,039
DPP U116_C	0,15	255,39	29,82	0,011
DPP U116_D	0,12	251,00	30,16	0,009
DPP U116_E	0,02	211,16	26,01	0,001

The optimum concentration at which the highest efficiency of DPP U116 was obtained was DPP:PCBM 3:2. Increase of photocurrent in comparison with DPP U115 is most likely caused by substitution of thiophene, which due to the induced mlecullar planarity and

resulting higher absorption and bathochromic shift leads to increased photocurrent. Results are shown in Table 12.

2.4.4 Discussion

The photovoltaic parameters of the solar cells prepared from the DPP U115 and DPP U 116 shows that the main difference is in the J_{sc}. The DPP U116 led to solar cells with two orders of magnitude higher J_{sc} than DPP U115. This is probably caused mainly due to much better absortion profile of the DPP U116. It nas beed showed that this is mainly caused by the more planar structure of the molecule that is caused by the thienyl. This improves the effective conjugation and thus reduces the optical band-gap. The other parameters (V_{oc} and FF) were, appart of some extremes values, nearly the same. This implies that the energy of the HOMO and LUMO were not that much affected by the change of the molecule structure.

2.5 SUMMARY

Goal of work was study the effect of the chemical structure of DPP on the optical properties. Four modifications were observed. Two had N- substituted aliphatic hydrocarbon and two samples were substituted N- dinitrophenyl. It has always been one version of the sample with a phenyl or thiophene.

Samples were studied with regard to the parameters required for the production of photovoltaic cells. First, they have been studied solubility. Already there are samples DPP and the DPP U117 U118 showed no absolutely ideal for continuation.

Further properties of the samples were studied in solution. They were measured by their optical properties such as absorption and fluorescence. Were measured to their maximum absorption, the absorption edge and was calculated max. abs. coefficient. The results were determined by emission spectra, max. emissions and Stokes shift was calculate. It was found that a substituted thiophene, which is more planar than phenyl, shifts the absorption to higher wavelengths. This led to the higher values of max. abs. coefficient.

The ability to form a good thin film is a key factor for OPV, therefore thin layer were prepared by spin coating. They were measured first by profilometer and found that due to the poor solubility of samples DPP U117 and DPP U118 did not form film sufficient. Thin layers of the prepared samples were also photographed under microscope. Then, thermal annealing was performed and it was found that the highest absorbance of thin layer was after tempering at 80 °C for DPP(TBFu)$_2$, DPP U115 and at 100 ° C for DPP U116. When comparing the results of optical properties of thin films and solutions it was found that absorption was for samples DPP(TBFu)2 and DPP U116 shifted to higher wavelengths. Emission spectra were for sample DPP U115 shifted to higher wavelengths and sample DPP U116 to lower wavelengths. It was due to the increase of crystallinity at thin layer against solution.

As a final step were prepared photovoltaic cells. For the reference sample DPP(TBFu)$_2$ was reached 3,3 % of the possible efficiency of 4 %. For samples DPP U115 and the DPP U116 was created concentration range with different concentrations of PCBM. The highest measured efficiency for a sample DPP U115 was 0,000 64 % and 0,04 % U116 DPP which confirms the conclusions evaluated during work.

SOURCES

[1] Why Solar?. ENGINEERING COM: Why Solar? [online]. [cit. 2015-01-03]. Dostupné:http://www.engineering.com/SustainableEngineering/RenewableEnergyEngineering/SolarEnergyEngineering/WhySolarEnergy/tabid/3893/Default.aspx

[2] Wikipedia: the free encyclopedia [online]. San Francisco (CA): Wikimedia Foundation, 2001-, 21. 10. 2014 v 21:44. [cit. 2015-01-03].

[3] SIGMA- ALDRICH: Organic photovoltaic. [online]. [cit. 2015-03-14]. Dostupné z:http://www.sigmaaldrich.com/materials-science/organic-electronics/opv-tutorial.html

[4] CAO, Weiran a Jiangeng XUE. Recent progress in organic photovoltaics: device architecture and optical design. *Energy*. 2014, vol. 7, issue 7, s. 2123-. DOI: 10.1039/c4ee00260a.

[5] HEEGER, Weiran a Jiangeng XUE. Recent progress in organic photovoltaics: device architecture and optical design. *Advanced Materials*. 2014, vol. 26, issue 1, s. 2123-. DOI: 10.1002/adma.201304373

[6] SCHARBER, M.C. a N.S. SARICIFTCI. Efficiency of bulk-heterojunction organic solar cells: Bulk Heterojunction Solar Cells. *Progress in Polymer Science*. 2013, vol. 38, issue 12, s. 1929-1940. DOI: 10.1016/j.progpolymsci.2013.05.001

[7] TANG, C. W. a N.S. SARICIFTCI. Two-layer organic photovoltaic cell: Bulk Heterojunction Solar Cells. *Applied Physics Letters*. 1986, vol. 48, issue 2, s. 183-. DOI: 10.1063/1.96937

[8] YANG, Fan, Max SHTEIN a Stephen R. FORREST. Controlled growth of a molecular bulk heterojunction photovoltaic cell: Bulk Heterojunction Solar Cells. *Nature Materials*. 2004-12-12, vol. 4, issue 1, s. 37-41. DOI: 10.1038/nmat1285.

[9] JANSSEN, René A. J. a Jenny NELSON. Factors Limiting Device Efficiency in Organic Photovoltaics. Advanced Materials. 2013-04-04, vol. 25, issue 13, s. 1847-1858. DOI: 10.1002/adma.201202873.

[10] WALKER, Bright, Jianhua LIU, Chunki KIM, Gregory C. WELCH, Jin Keun PARK, Jason LIN, Peter ZALAR, Christopher M. PROCTOR, Jung Hwa SEO, Guillermo C. BAZAN a Thuc-Quyen NGUYEN. Optimization of energy levels by molecular design: evaluation of bis-diketopyrrolopyrrole molecular donor materials for bulk heterojunction solar cells. Energy. 2013, vol. 6, issue 3, s. 952-. DOI: 10.1039/c3ee24351f.

[11] B. Walker, C. Kim and T.-Q. Nguyen, Chem. Mater., 2011, 23, 470.

[12] LIU, Jianhua, Bright WALKER, Arnold TAMAYO, Yuan ZHANG a Thuc-Quyen NGUYEN. Effects of Heteroatom Substitutions on the Crystal Structure, Film Formation, and Optoelectronic Properties of Diketopyrrolopyrrole-Based Materials. Advanced Functional Materials. 2013-01-07, vol. 23, issue 1, s. 47-56. DOI: 10.1002/adfm.201201599.

[13] PFLEGER, J.: Polymerní nanostruktury v optoelektronice. Otevřená věda: Praktické kurzy z fyziky a chemie. Akademie věd české republiky, 2006.

[14] NUNZI, Jean-Michel. 2002. Comptes Rendus Physique. 3(4). DOI: 10.1016/S1631-0705(02)01335-X. ISSN 16310705.

[15] QU, Sanyin a He TIAN. Diketopyrrolopyrrole (DPP)-based materials for organic photovoltaics.Chemical Communications. 2012, vol. 48, issue 25, s. 3039-. DOI: 10.1039/c2cc17886a.

[16] PEUMANS, Peter, Soichi UCHIDA a Stephen R. FORREST. 2003-9-11. efficient bulk heterojunction photovoltaic cells using small-molecular-weight organic thin films. Nature.425(6954): 158-162. DOI: 10.1038/nature01949. ISSN 0028-0836.

[17] *Praktikum z fyziky I.: Měření účinnosti přeměny (konverze) fotovoltaického článku* [online].[cit.2015-05-18]. Dostupné z: https://www.vutbr.cz/elearning/mod/resource/view.php?id=256198

LIST OF ABBREVIATION AND SYMBOLS

BHJ	bulk hetero-junction
FF	fill factor
eq.	equation
em.	emission
ex.	excitation
η	efficiency
FMO	fragment molecular orbital
D	donor
A	acceptor
DPP	diketopyrrolopyrrole